

AGE-DEPENDENT MORPHOLOGICAL AND COMPOSITIONAL VARIATIONS ON CERES.

R. Jaumann^{1,2}, K. Stephan¹, K. Krohn¹, K.-D. Matz¹, K. Otto¹, W. Neumann¹, T. Kneissl², N. Schmedemann², S. Schroeder¹, F. Tosi³, M.C. De Sanctis³, F. Preusker¹, D. Buczowski⁴, F. Capacioni³, U Carsenty¹, S. Elgner¹, I. von der Gathen¹, T. Giebner¹, H. Hiesinger⁵, M. Hoffmann⁶, E. Kersten¹, J.-Y. Li⁷, T.B. McCord⁸, L. McFadden⁹, S. Mottola¹, A. Nathues⁶, A. Neesemann², C. Raymond¹⁰, T. Roatsch¹, C. T. Russell¹¹, B. Schmidt¹², F. Schulzeck¹, R. Wagner¹, D. A. Williams¹³; ¹DLR, Institute of Planetary Research, Berlin, Germany (ralf.jaumann@dlr.de); ²Freie Universität Berlin, Germany; ³Istituto di Astrofisica e Planetologia Spaziali, INAF, Roma, Italy; ⁴Johns Hopkins University Applied Physics Laboratory, Laurel, MD, USA; ⁵Westfälische Wilhelms-Universität Münster, Germany; ⁶MPI for Solar System Research, Göttingen, Germany; ⁷Planetary Science Institute, Tucson, AZ, USA; ⁸Bear Fight Institute, Winthrop, WA, USA; ⁹NASA Goddard Space Flight Center, Greenbelt, MD, USA; ¹⁰Jet Propulsion Laboratory, California Institute of Technology, Pasadena, CA, USA; ¹¹UCLA, Institute of Geophysics, Los Angeles, CA, USA; ¹²Georgia Institute of Technology, Atlanta, GA, USA; ¹³Arizona State University, Tempe, TX, USA;

Introduction: The potential presence of ice within Ceres' crust [1] raises the prospect of geological processes similar to differentiated icy bodies [2]. Stereophotogrammetric analysis of Ceres yields an overall relief from -7.5km to 7.5km. The observed relief to size ratio of 3.6% is high compared to other icy bodies, indicating crustal dynamics and related steep slopes. Pre-Dawn telescopic observations suggest some aqueous alteration, including the formation of clay-like materials [e.g. 3], and possibly salts incorporated into a regolith layer of small-scale compositional variations [1,4]. Thermal models suggest that Ceres is at least partially differentiated and could have undergone tectonic and cryovolcanic processes [1,4,5]. The potential for a relatively thin hydrosphere on Ceres [12,4] could give rise to a connection between endogenic activity and surface features.

Geological Setting: Extended smooth plains cover the interior of a number of craters. Prominent examples are Ikapati, Occator and Haulani (Fig.1).

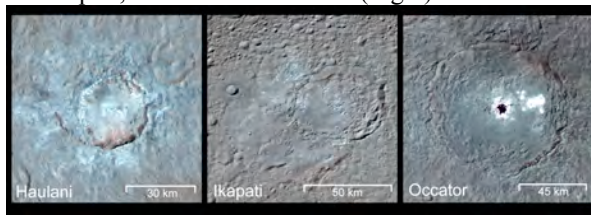


Fig. 1 HAMO observations of the distribution of bluish and brownish/reddish material in and around the impact crater Haulani, Ikapati and Occator.

Ikapati shows smooth plains on different topographic levels associated with pits and flow-like features that overrun crater rims. The material forming these plains, ponds in depressions and smaller craters and cover the pre-existing surface creating a distinct geological boundary. The interior of Occator also exhibits extended plains of ponded material, multiple flows originating from the center overwhelming the mass wasting deposits from the rim, dome-like features, vents cracks and fissures (Fig.2). Furthermore, crater densities on Occator's floor are lower than those on the ejecta blanket indicating a post-impact formation age of the flows (Fig.4). The flows to the northeast appear to originate

from the central region and move slightly uphill. This indicates either a feeding zone that pushes the flows forward by supplying low-viscosity material or a depression of the crater center, possibly after discharging a subsurface reservoir.

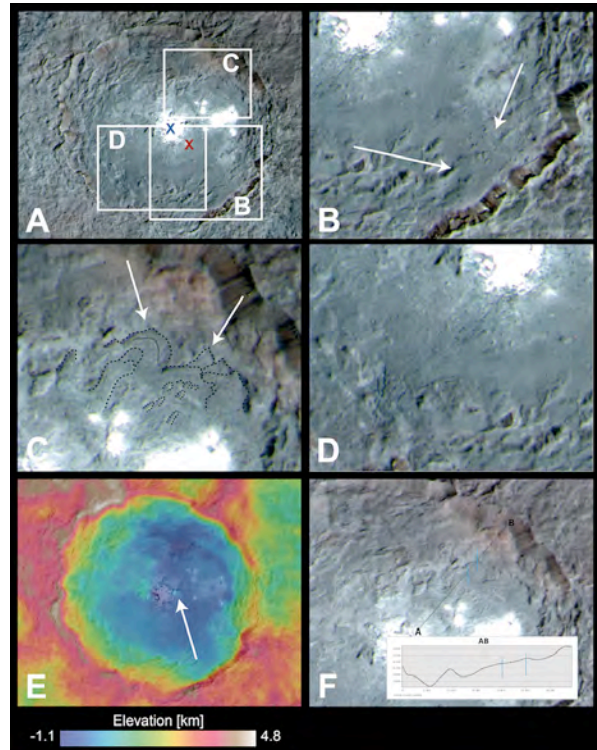


Fig. 2 Occator crater (239.2°E/19.7°S). Surface temperatures: blue 'X'=217K, red 'X'=228K (image width 119 km). B) Extended plains of ponded material cover mass wasting deposits and pile up at crater walls (arrows) (image width 62.5 km). C) Flows spread out from the central white spots and flow fronts collide with mass wasting deposits; superimposed individual flows (arrows) indicate multiple flow events (image width 36 km). D) Extension cracks extending from a hummocky area between flooded slumping blocks and spreading radially with a partly polygonal pattern (image width 27 km). E) Digital terrain model of Occator. F) Cross section from the center along the flow features.

Haulani crater also exhibits interior smooth plains with flow features originating from a mountainous region in the center ponding towards mass wasting deposits from

the rim. Haulani also shows flows running from the crater rim outwards to the surrounding area covering the pre-existing surface as indicated by an obvious geological boundary similarly to the observation in the Ikapati region.

Compositional constrains: In the enhanced color images (Fig.1) the plains and flows as well as some areas surrounding the craters appear spectrally blue. Both plains and flow material in Occator, Haulani and Ikapati are characterized in FC and VIR visible spectra by a slightly negative slope with a gradual drop off up to 10% in reflectance from 0.5 μ m to 1 μ m (Fig.3).

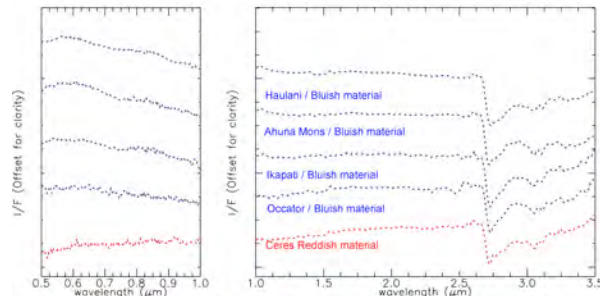


Fig. 3 Spectral characteristics of bluish material in Haulani, Ikapati, Occator and Ahuna Mons for comparison. Bluish material is up to 3 times brighter than the average. The spectra of the bluish material show a steeper 0.5 to 0.9 μ m gradual drop off than the average Ceres spectra. The 0.72 μ m absorption might be due to radiation-induced color variations [6] in salts is well exposed in all spectra. Bands at 2.7 and 3.06 μ m are due OH in phyllosilicates and ammonium [7]. Although the spectral variations in the visible are subtle, they are clearly expressed in the color ratio composite (Fig.4). A drop off in reflectance across the visible is also observed on several B-type asteroids and is commonly modeled by various carbonaceous chondrite meteorites [8]. However, these meteorites are composed of silicates (olivine, pyroxene) rather than ammoniated phyllosilicates [7] as Ceres. An increased reflectivity peaking in the blue spectral range has been reported from icy satellites and suggested to possibly be due to Rayleigh scattering induced by nanophase iron on icy surfaces as a result of weathering and/or contamination [9]. Rayleigh scattering characterized by a strong peak at blue wavelength and a very strong non-linear drop in reflectance towards 1 μ m does not fit the gradual linear drop of reflectance of Ceres. Multiple scattering might be another explanation, however, Ceres' average spectrum is neutral and adding white material to a spectrally neutral surface will just increase albedo but not change the slope. Particle size variations might also be an explanation but to cause such an effect significant size differences have to be expected [8] which would cause effects in the infrared that are not observed [10]. However, a negative slope with a gradual drop from 0.5 μ m to 1 μ m, resulting in a bluish appearance of the surface, can also be caused by

a component of salts, either sulfates [11] and/or chlorates [12, 13].

Age correlation: The crater densities of 20 locations across the surface of Ceres were analyzed in order to investigate the age dependence of spectral surface features. The results indicate that the bluish material is mainly associated with the youngest impact craters on Ceres (< 0.5 Ga) (Fig.4). The investigated craters located in the reddish/brownish regions are typically much older (> 1 Ga) (Fig.3), suggesting that the bluish material changes its spectral characteristics with time either due to weathering, radiation, particle size decrease or compositional alteration like dehydration.

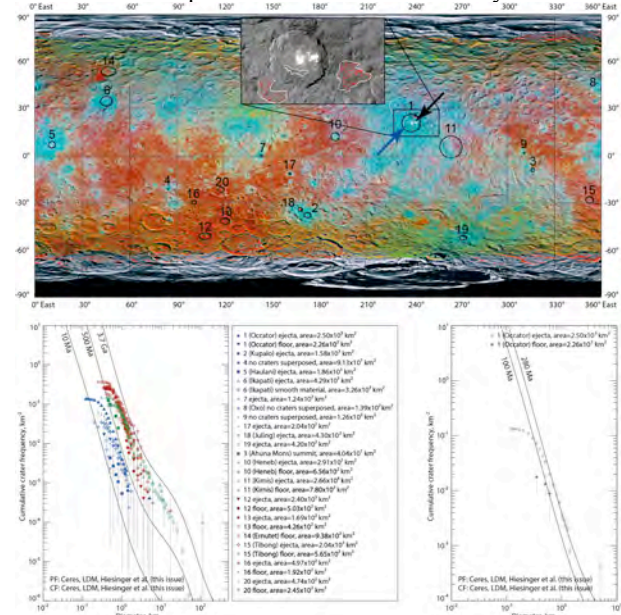


Fig. 4. Top: Locations (numbers) of investigated impact craters superposed on a global color-ratio mosaic. Lower left: CSFD measured on crater floors and continuous ejecta blankets. Reddish and bluish symbols correspond to the surface color in top map. Greenish symbols represent features where the source of the bluish material is unclear. Lower right: CSFD measured on the crater floor as well as on continuous ejecta blankets of Occator (insert in top map).

References: [1] T.B. McCord, C. Sotin, Ceres: *J. Geophys. Res.* **110**, E05009 (2005). [2] P.C. Thomas, *et al.*, *Nature* **437**, 224–226 (2005). [3] A.S. Rivkin, *et al.*, *Space Sci. Rev.* **163**, 95–116 (2011). [4] J.C. Castillo-Rogez, T.B. McCord, *Icarus* **203**, 443–459 (2010). [5] T.B. McCord, J. Castillo-Rogez, A. Rivkin, *Space Sci. Rev.*, **163**, 63–76 (2011). [6] K.P. Hand and R.W. Carlson, *Geophys. Res. Lett.*, **42**, 3174–3178. [7] M.C. De Sanctis, *et al.*, *Nature*, **528**, 241–244, (2015) [8] B.E. Clark *et al.*, *J. Geophys. Res. Planets* **115**, E06005, (2010). [9] R.N. Clark, *et al.*, *Icarus* **193**, 372–386 (2008). [10] E. Ammannito *et al.*, *Science* (2016) submitted. [11] Nathues *et al.*, *Nature*, **528**, 237–240. (2015). [12] J. Hanley, *et al.*, *J. Geophys. Res. Planets* **120**, 1415–1426 (2015). [13] L. Ojha, *et al.*, *Nat. Geosci.* advance online publication (2015). [13] J. Bishop *et al.*, *Phil. Trans. R. Soc. A* **372**, 20140198, (2014).